Supporting Information

Graphene/Carbon-dot Hybrid Thin Films Prepared by a Modified Langmuir-Schaefer Method

Antonios Kouloumpis,[1,2] Eleni Thomou,[1] Nikolaos Chalmpes,[1] Konstantinos Dimos,[1] Konstantinos Spyrou,[1] Athanasios B. Bourlinos,[3] Ioannis Koutselas,[4] Dimitrios Gournis[1] and Petra Rudolf[2]**

[1] Department of Materials Science and Engineering, University of Ioannina, GR-45110 Ioannina, Greece

[2] Zernike Institute for Advanced Materials, University of Groningen, Nijenborgh 4, NL-9747AG Groningen, the Netherlands

[3] Physics Department, University of Ioannina, Ioannina GR-45110, Greece

[4] Department of Materials Science, University of Patras, GR-26504 Patras, Greece

Experimental procedures

Preparation of hydrophobic quartz substrates

The surface modification of hydrophilic quartz substrates (Sigma Aldrich) achieved by a one-step Langmuir Schaefer (LS) deposition in a Langmuir Blodgett (LB) trough. Ultrapure water was used as subphase and octadecylamine (99%, ODA, Sigma Aldrich) (0.2 mg mL^{-1}) dissolved in chloroform/methanol 9/1 (v/v) was spread onto the surface with the help of a microsyringe. The hydrophilic quartz was dipped horizontally (LS method) at a constant surface pressure of 30 mN m^{-1} as shown in Figure S1. After the LS deposition, the quartz substrate was rinsed with pure water and dried with a flow of N_2 gas.

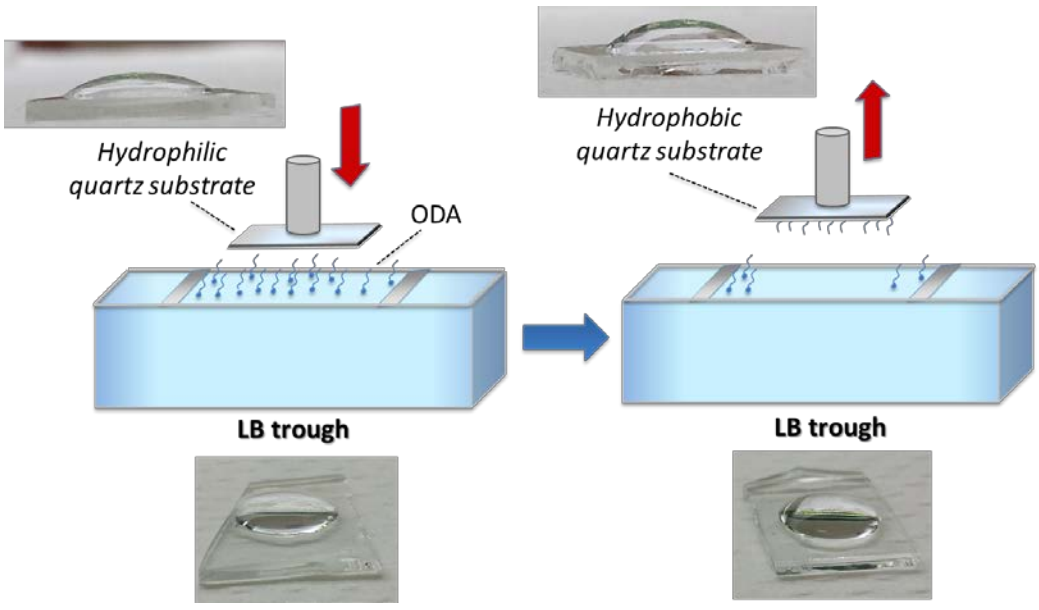

Figure S1. Schematic representation of surface modification of hydrophilic quartz substrates

Deposition of isolated C-dots on Si-wafers for the AFM measurements

Isolated pristine C-dots deposited on Si-wafers (Si-Mat) were obtained by a technique which combines Langmuir-Schaefer deposition and self-assembly[1-3]. Ultrapure water was used as subphase in the LB trough and a stearic acid (99%, Fluka) (0.2 mg mL^{-1}) dissolved in chloroform-methanol (9:1) was spread onto the aqueous subphase with the help of a microsyringe. A hydrophobic Si-wafer was dipped horizontally in the air-water surface (LS method) at a constant surface pressure of 15 mN m^{-1}. After the LS deposition, the substrate was rinsed with pure water and dipped into an aqueous dispersion (0.2 mg mL^{-1}) of C-dots as shown in Figure S2. Finally, the surface was rinsed copiously with pure water and dried with a flow of N_2 gas.

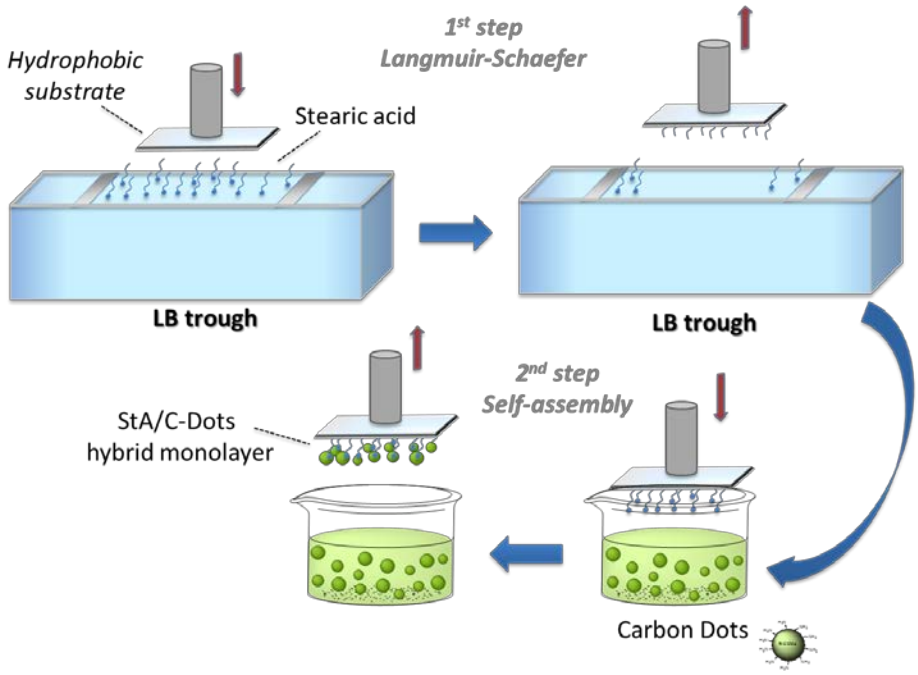

Figure S2. Schematic representation of the synthetic procedure for the deposition of isolated C-dots on a hydrophobic Si-wafer

Characterization of pristine C-dots

The X-ray diffraction pattern of the produced C-dots (in powder) is shown in Figure S3. The broad peak at ~25° with a d-spacing of 3.5 Å corresponds to highly disordered carbon atoms, similar to the graphite lattice spacing [4-7].

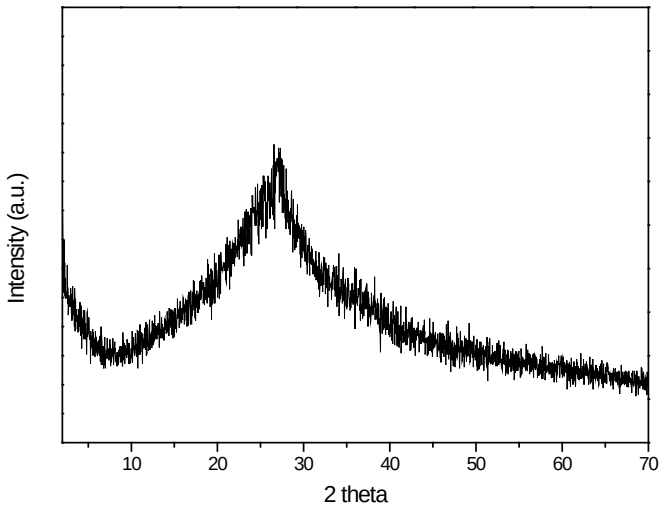

Figure S3. X-ray diffraction pattern of pristine C-dots

FT-IR was used in order to identify the functional groups on the surface of the carbon dots (in powder) (Figure S4). The broad absorption band at 3000-3500 cm^{-1} is attributed to the stretching vibrations of O–H and N–H. The absorption bands at 1600 and 1710 cm^{-1} are attributed to the stretching vibrations of C=O, whereas those at 1405 and 1355 cm^{-1} to the bending vibrations of CH_2. Finally, the band located at 1055 cm^{-1} is attributed to the stretching vibrations of C-O-C. [4, 8-9]

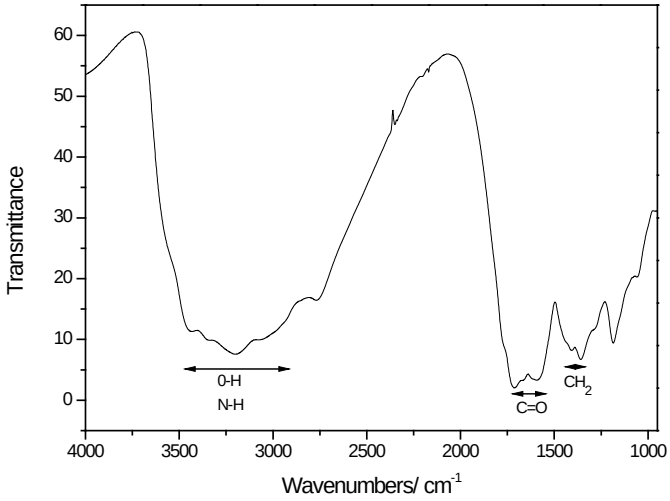

Figure S4. FT-IR spectrum of pristine C-dots

The UV-vis spectrum (Figure S5) of an aqueous dispersion of the carbon dots (0.2 mg mL^{-1}) is comparable to previous literature reports[4] and consists of two main absorption bands at 340 and 405 nm.

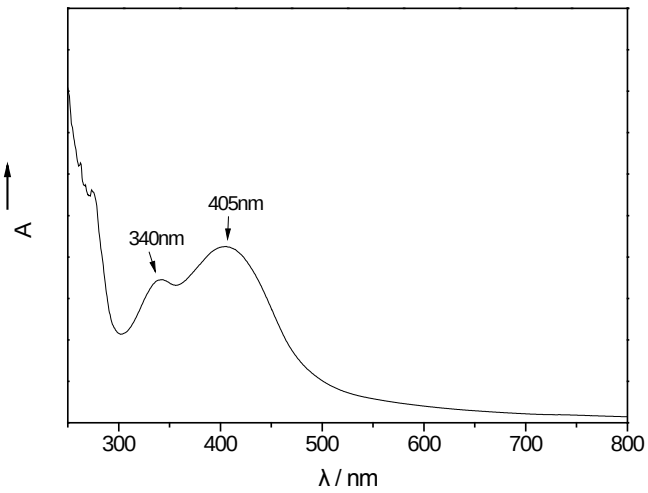

Figure S5. UV-Vis spectrum of an aqueous dispersion of C-dots

The Raman spectrum (Figure S6) of the pristine C-dots (in powder) displays the characteristic D and G bands that are attributed to the sp^3 and sp^2 hybridized carbon atoms respectively. The relative intensity (I_D/I_G) for the C-dots is equal to 0.95.

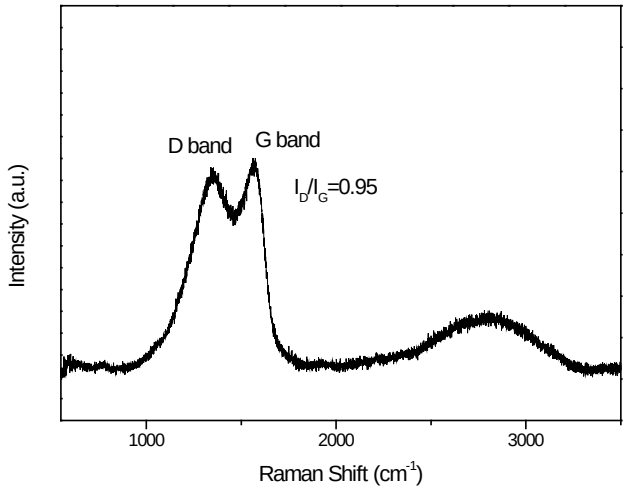

Figure S6. Raman spectrum of pristine C-dots

The C1s photoelectron spectrum of carbon dots (Figure S7 left) consists of three peaks. The first one at a binding energy of 284.6 eV is attributed to the C-C and/or C-H bonds (66.7% of the total C1s spectral intensity), the second one at 286.2 eV to C-O and C-N bonds (21.0 %) while the last peak at 288.0 eV arises from the C=O bonds and constitutes 12.3 % of the spectral intensity. The N1s photoelectron spectrum of carbon dots (Figure S7 right) is deconvoluted into two photoelectron peaks, one at 399.8 eV binding energy,[10] which is attributed to the amine groups and a second one at 401.5 eV due to protonated amines of the C-dots. The atomic percentage of carbon, nitrogen and oxygen atoms is reported in Table below.

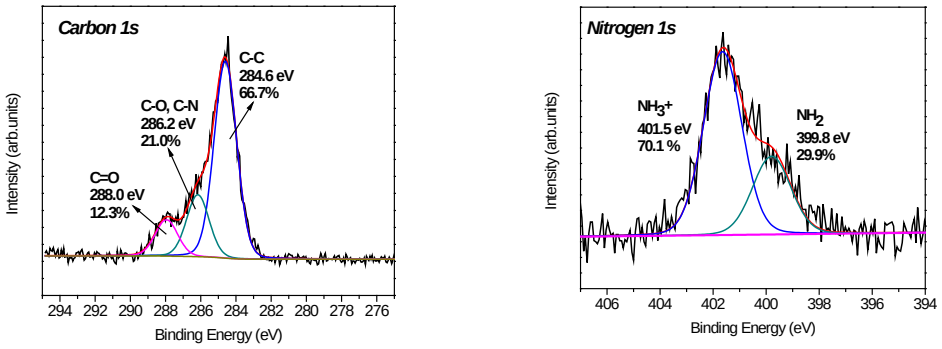

Figure S7. C1s (left) and N1s (right) core level X-ray photoemission spectra of carbon dots

	Atomic Percentage %	Error %
Carbon	63.5	2.5
Oxygen	29.0	0.6
Nitrogen	7.5	0.7

Finally, images of aqueous dispersion of C-dots under normal light and UV illumination at 254 nm and 365 nm are shown in Figure S8. Analogous optical and fluorescent images of C-dots deposited on a commercial filtration paper are shown in Figure S9.

Figure S8. Images of an aqueous dispersion of C-dots with room lights on (left), room lights off but UV illumination on at 254 nm (center) and 365 nm (right).

Figure S9. Images of C-dots deposited on an available commercial filtration paper with room lights on (left), room lights off but UV illumination at 254 nm (center) and 365 nm (right).

II-α isotherms and morphological characterization of ODA-GO monolayers

To prove that ODA and GO flakes bind, we recorded the surface pressure- area (∏-a) isotherms while compressing the Langmuir films by means of the movable barriers of the LB trough. Figure S10 displays the ∏-a isotherms of an ODA monolayer on pure water and on GO in various dispersions. For each curve changes in slope are observed when the floating layer goes through a phase transition during

the compression process: two dimensional gas to liquid and then liquid to solid. For the ODA layer on pure water the phase transition gas-liquid is observed at a much higher surface pressure than for ODA on the GO suspension because when GO has covalently bound via the amide functionality of ODA, the GO platelets in hybrid floating layer of ODA-GO start to interact at much lower pressures than where the ODA molecules feel each other strongly enough to form a two dimensional liquid. In other words, the difference in surface pressure where the gas-liquid transition occurs in the Langmuir film is a proof for the successful grafting of GO to ODA.[4]

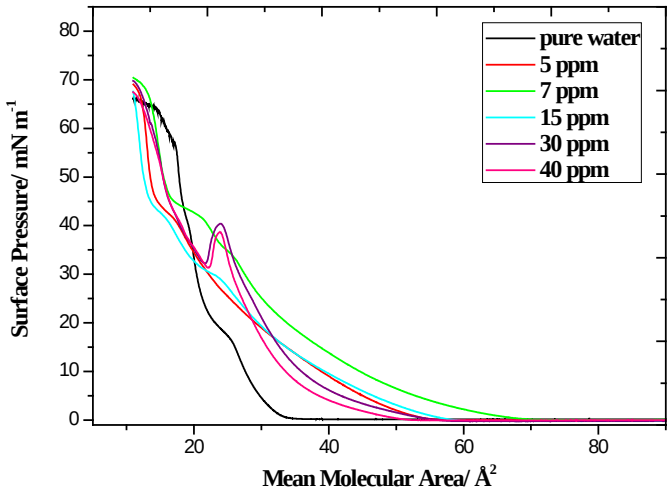

Figure S10. ∏-a isotherms recorded during the compression of ODA monolayers on pure water and on various aqueous dispersions of GO.

Representative AFM images of the hybrid Langmuir monolayers (ODA-GO) deposited on Si-wafer at different points of the recorded Π–a isotherms (surface pressures of 5, 10, 15 and 20 mN m^{-1}) are shown in Figure S11. The topographic images revealed that the substrate surface coverage of the hybrid ODA-GO monolayers is higher as the surface pressure increases. Homogeneous GO nanosheets with well-defined edges are easily observed in the AFM micrographs, verifying the

effectiveness of LB method in terms of coverage, uniformity and single-layer level control.

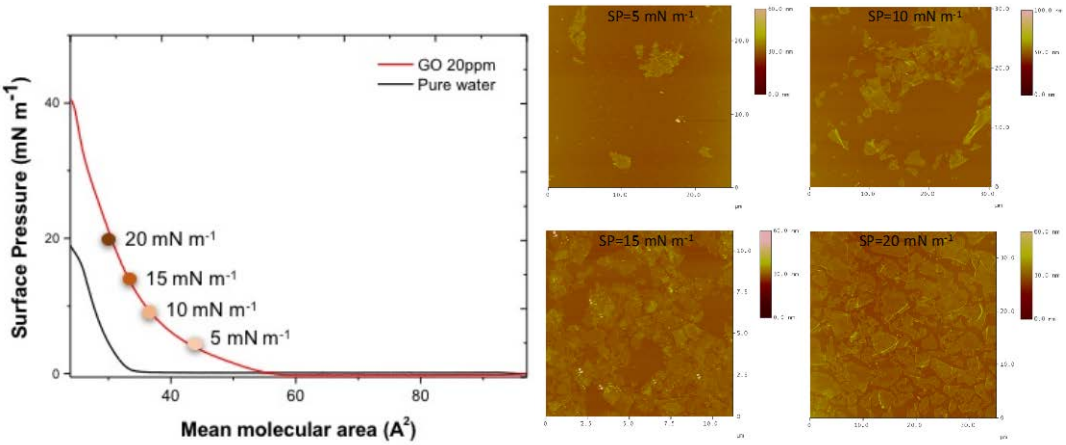

Figure S11. AFM height images of the floating ODA-GO monolayer deposited on Si-wafer substrates at different surface pressures.

References

1. Bourlinos, A. B.; Trivizas, G.; Karakassides, M. A.; Baikousi, M.; Kouloumpis, A.; Gournis, D.; Bakandritsos, A.; Hola, K.; Kozak, O., et al., Green and Simple Route toward Boron Doped Carbon Dots with Significantly Enhanced Non-Linear Optical Properties. *Carbon* **2015,** *83*, 173-179.

2. Bourlinos, A. B.; Georgakilas, V.; Bakandritsos, A.; Kouloumpis, A.; Gournis, D.; Zboril, R., Aqueous-Dispersible Fullerol-Carbon Nanotube Hybrids. *Materials Letters* **2012,** *82*, 48-50.

3. Bourlinos, A. B.; Bakandritsos, A.; Kouloumpis, A.; Gournis, D.; Krysmann, M.; Giannelis, E. P.; Polakova, K.; Safarova, K.; Hola, K., et al., Gd(Iii)-Doped Carbon Dots as a Dual Fluorescent-Mri Probe. *J. Mater. Chem.* **2012,** *22* (44), 23327-23330.

4. Qu, S.; Wang, X.; Lu, Q.; Liu, X.; Wang, L., A Biocompatible Fluorescent Ink Based on Water-Soluble Luminescent Carbon Nanodots. *Angewandte Chemie International Edition* **2012,** *51* (49), 12215-12218.

5. Peng, H.; Travas-Sejdic, J., Simple Aqueous Solution Route to Luminescent Carbogenic Dots from Carbohydrates. *Chem. Mater.* **2009,** *21* (23), 5563-5565.

6. Zhou, J.; Booker, C.; Li, R.; Zhou, X.; Sham, T.-K.; Sun, X.; Ding, Z., An Electrochemical Avenue to Blue Luminescent Nanocrystals from Multiwalled Carbon Nanotubes (Mwcnts). *Journal of the American Chemical Society* **2007,** *129* (4), 744-745.

7. Yang, Y.; Cui, J.; Zheng, M.; Hu, C.; Tan, S.; Xiao, Y.; Yang, Q.; Liu, Y., One-Step Synthesis of Amino-Functionalized Fluorescent Carbon Nanoparticles by Hydrothermal Carbonization of Chitosan. *Chem. Commun.* **2012,** *48* (3), 380-382.

8. Himaja, A. L.; Karthik, P. S.; Singh, S. P., Carbon Dots: The Newest Member of the Carbon Nanomaterials Family. *The Chemical Record* **2015,** *15* (3), 595-615.

9. Xu, M.; He, G.; Li, Z.; He, F.; Gao, F.; Su, Y.; Zhang, L.; Yang, Z.; Zhang, Y., A Green Heterogeneous Synthesis of N-Doped Carbon Dots and Their Photoluminescence Applications in Solid and Aqueous States. *Nanoscale* **2014,** *6* (17), 10307-10315.

10. Moulder, J. K.; Stickle, W. F., *Handbook of X-Ray Photoelectron Spectroscopy*. Physical Electronics, Inc.: 1995.